RESEARCH ARTICLE

Wind turbine sensor array for monitoring avian and bat collisions†

Congcong Hu,[1] Roberto Albertani,[1] and Robert M. Suryan[2,3]

[1] *School of Mechanical, Industrial and Manufacturing Engineering, Oregon State University, Corvallis, Oregon, USA*
[2] *Department of Fisheries and Wildlife, Oregon State University, Hatfield Marine Science Center, Newport, Oregon, USA*
[3] *Current address: NOAA Fisheries, Alaska Fisheries Science Center, Auke Bay Laboratories, Ted Steven's Marine Research Institute, Juneau, Alaska, USA*

Correspondence: R. Albertani, School of MIME, Oregon State University, Corvallis, Oregon, USA.
Email: roberto.albertani@oregonstate.edu

Received June 6 2017; Revised October 25 2017; Accepted XXX

Abstract

Assessment of avian and bat collisions with wind turbines is necessary to ensure that the benefits of renewable wind power generation are not outweighed by mortality of protected species. An onboard, integrated multi-senor system capable of providing detection of turbine collision events, including taxonomic information, was developed. The conceptual design of a multi-sensor system including a vibration sensing node, an optics node, and an bioacoustic node with an event-driven trigger architecture was field-tested on utility-scale wind turbines. A pixel density computational model was built to estimate the spatial coverage and target resolution to the optimized configuration for camera placement. Field test results of the vibration node showed that nearly half of the recorded impact events were successfully identified by visual inspection and running short-time Fourier transform on recorded vibration signals. The remaining undetected impact events were masked under background noise due to low impact energy and high background noise of the operating turbine which result in subsequent low signal-to-noise ratio. Our results demonstrate the feasibility of triggering the system through single impact event sensed by vibration sensors.

Keywords: wind turbine; birds; bats; environment; vibration sensors; impact monitoring

1 Introduction

In recent years, wind energy generation is experiencing rapid worldwide development and is expected to play a significant role in the coming decades. In the United States, a total gross offshore wind energy potential of 4150

†This document is prepared using WileyNJD-v1.cls.

gigawatts (GW) was estimated by the National Renewable Energy Laboratory (NREL) (1). However, the deployment of offshore wind farms brings environmental concerns such as interactions with marine life, increased noise, alterations to food resources, and disturbance to the seabed (2). One of the major ecological concerns is the potential threat to marine bird species due to collisions with wind turbines (3, 4). Studies of bird and bat mortality rates for collisions with utility-scale wind turbines have reported an estimate of up to 40 deaths per turbine per year on certain sites (5, 6). It is imperative that the development of offshore wind facilities will include efforts to minimize negative impact on bird and bat species, especially those that are listed as endangered or threatened.

Common methodologies applied at land-based wind farms for bird/bat collision assessments and mortality rate monitoring are carcass survey and long-term visual observation (7), made generally at the scale of a single wind farm. Due to surveyor efficacy and carcass removal by scavengers, the count could be inaccurate, and the true magnitude of the problem could be underestimated. Most importantly, carcass surveys are expensive or infeasible at some sites, such as agricultural fields, dense shrub habitats, remote locations, and offshore. Common methodologies used to estimate potential interactions with offshore wind facilities are visual surveys (aerial and boat based), radar monitoring, and acoustic recordings that can inform collision risk models based on flux data (8–13). Although these methodologies are powerful tools for the assessment of displacement effects of local birds and barrier effects of the wind farms on birds during migration, they are poorly suited for directly monitoring of collision events with wind turbines. Hence, effective and low-cost methods of collision event monitoring are required. Such approaches should include on-board systems with automatic collision detection, provide information for taxonomic identification, feature automatic monitoring, and ensure a long operational life with minimum maintenance.

One approach for automatic detection of bird/bat collision with wind turbines is abnormal event monitoring by the implementation of vibrational or acoustic sensing devices. Vibration-based monitoring techniques are well developed and widely adopted by modern wind turbines for rotating parts (e.g. blades, bearings, gearbox) (14). Vibration sensors such as piezoelectric accelerometers are commonly installed on wind turbines for the analysis of dynamic structural response during operations (15, 16). The WT-bird bird collision monitoring system (17) initially employed wired contact microphones (piezoelectric transducers sensitive to sound propagating through solid structures) on the blades before switching to wired accelerometers to improve durability and signal-to-noise ratios. Results have confirmed the feasibility of detection of collision events from structural vibration signals. Another approach, video surveillance (in either visual or infrared spectrum), also is widely employed by avian species monitoring systems. One notable infrared-based monitoring system is the Thermal Animal Detection System (TADS) (18), which was developed and applied to identify species through wing beat analysis and animal size. However, its collision detection function is not automatic, and a manual review of all collected imagery is required to assess the interactions of volant species with wind turbines.

Based on prior bird collision monitoring systems, this paper presents the conceptual design of a multi-sensor system that provides both temporal and spatial coverage capacities for auto-detection of bird collision events. Field testing was performed on utility-scale wind turbines. Testing details such as device positioning and sensor selection on the application of two main types of integrated vibration sensors (i.e. accelerometer and contact microphone) are discussed. Artificial collision events were created by launching tennis balls into moving blades using compressed-air cannon. The objectives of this project are to test and evaluate signal qualities of common vibration sensors on non-stationary wind turbines to determine the feasibility of the designed multi-sensor system, and to serve as some basis to help develop advanced auto-detection systems for bird collision event monitoring in the future.

2 System description and testing

2.1 Multi-sensor system overview

The design of the on-board multi-sensor system under daylight operations mainly consists of four components: 1) the vibration sensor node (accelerometers and contact microphones) installed on the root of the blade, 2) the optical node (visual cameras) aiming at the rotor plane, 3) the bioacoustics node (acoustic microphones) mounted outside the nacelle, and 4) the data acquisition system and central controller inside the nacelle. The schematic diagram of the system is shown in Figure 1. The vibration sensors provide continuous vibration monitoring, while the optical and acoustic nodes acquire necessary information (i.e. visual images, impact sounds, and animal calls) for event confirmation and species recognition when an impact is detected. Since continuous data acquisition by the optical node at frame rates sufficient to capture fast-moving objects will produce a prohibitory volume of data to be archived, requiring massive post-processing, the event-driven trigger architecture has been developed to address this challenge. Each node continuously streams data into a ring buffer for temporary storage. When an event (e.g. collision) is registered by the vibration node, all buffers will store data in an operator-determined time window (e.g. equal temporal period of temporal data on both sides of a triggered event), and eventually, all buffered data will be asynchronously stored on disk. This architecture minimizes the volume of data archived, and enhances efficiency of data post-processing.

2.2 Vibration node

The sensing of blade vibrations was tasked as the primary triggering source for image acquisition and impact confirmation. As such, particular attention was devoted to testing two different sensors for the same function with the objective to ultimately select the more practical sensor. The two sensors were 1) wireless three-axis accelerometers (LORD MicroStrain G-Link LXRS w/ 104-LXRS base station), and 2) wireless contact microphones (Sun-Mechatronics

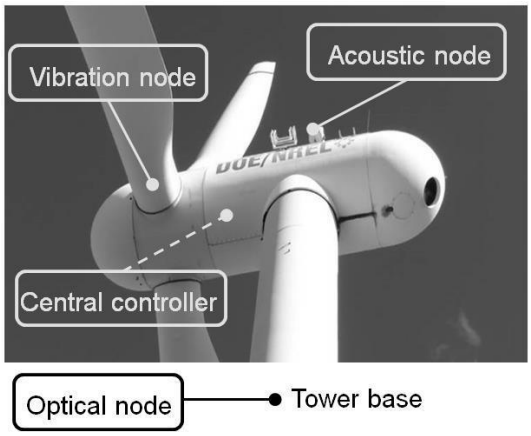

Figure 1: Schematic diagram of the auto-detect system with event-driven trigger architecture on NREL CART3 wind turbine.

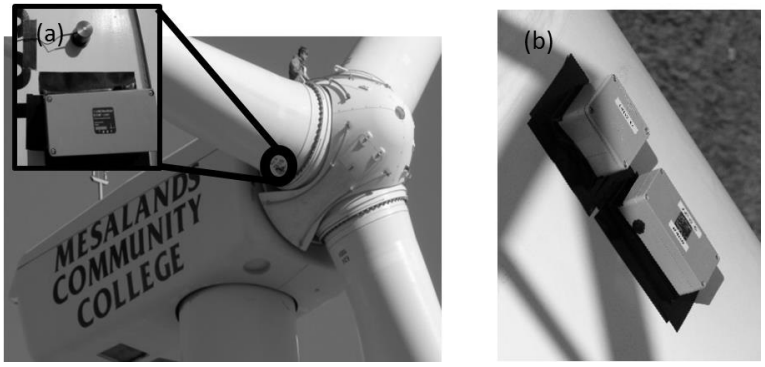

Figure 2: Sensor placement: vibration sensors mounted on the blade including (a) 1.5 MW GE wind turbine at NAWRTC (b) 600 kW CART3 wind turbine at NREL-NWTC.

USK-40 w/ UZ-10 UHF receiver). Two per blade, they formed the vibration node, providing continuous structural vibration monitoring and collision event trigger in the event-driven architecture. The sensors with weatherproof housing were installed at the root of the blades, as shown in Figure 2, for easier accessible installation, easy maintenance, and negligible aerodynamic effects on the blades. The blade surface first was cleaned at the application location, and the housing box was applied to the surface with proper orientation (one axis parallel to the longitudinal axis of the blade) using 3M double bonding tape. The accelerometer signal was digitized prior to wireless transmission, while the contact microphone signal was transmitted as an analog signal, and was digitized by a NI USB-4431 DAQ (www.ni.com) at the receiver station. The receiver station containing paired wireless receivers was placed inside the nacelle next to the central controller. For timely processing of data for real-time collision monitoring, considering the processing ability of current hardware (16), sampling rates were chosen at 512 Hz for accelerometers and 1000 Hz for contact microphones.

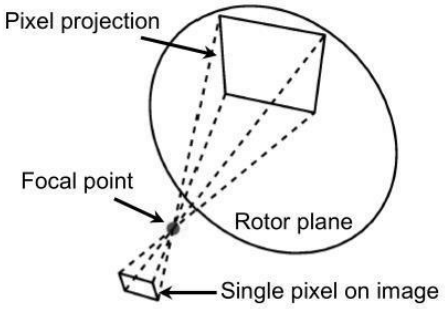

Figure 3: Illustration of pixel mapping.

2.3 Bioacoustics node

The bioacoustics node consisted of an acoustic microphone (G.R.A.S. general-purpose electronic piezoelectric microphone with frequency range of 10 to 20,000 Hz). The microphone was placed on top of the nacelle. In addition to species audio identification, it is valuable for environmental assessment that might lead to missed or false impact triggers (e.g. rain, lightning, etc.). Since no avian vocalizations were recorded due to the short timeframe of the testing, only acoustic recordings of turbine operation associated with an impact trigger used to trigger the system were collected, thus providing a proof of concept for an integrated bioacoustics node to be used as potential extra source of trigger.

2.4 Optical node

The implementation of optical cameras always involves the tradeoff between target resolution and field of view (FOV). In general, wider field of view would also result in lower target resolution. A target pixel density simulation model was developed to find the proper camera deployment location. With known camera specifications (i.e. effective focal length, sensor size, and image resolution), position (i.e. distance from camera to the rotor plane) and orientation, each pixel on the image can be projected (mapped) onto the rotor plane using trigonometric functions, as illustrated in Figure 3. For a given physical dimension on the rotor plane, the target resolution can be estimated as the sum of pixel pitches for all correlated pixels. Three options of optical node configurations are 1) on the nacelle, with a field of view that intersects the rotor plane, 2) on the turbine tower, near its base, in an upward-facing configuration, and 3) on an adjacent tower, viewing the entire rotor plane. During the field testing, option 2) was tested with a visual camera (Currera-R RL50C-OC) deployed near the tower base with an upper angle of view targeting the blade rotor plane, due to the short testing timeframe.

2.5 System field tests

The required sub component functions and overall system functionality, reliability, and accuracy had to be validated in field tests with operating wind turbines and simulated bird impacts on the blades. Two locations for tests were selected for availability of wind turbines not involved in commercial energy conversion and for the excellent technical and logistic support on site. Partial system early tests were performed at the North American Wind Research and Training Center (NAWRTC) at the Mesalands Community College in Tucumcari, NM. The Center operates a General Electric GE 1.5 MW wind turbine. Later tests on the fully integrated system were performed at the National Renewable Energy Laboratory (NREL) National Wind Technology Center (NWTC) in Boulder, CO. The turbine used at the NWTC was the 600 kW CART3 (three blades).

In both cases, bird impacts were simulated by launching tennis balls using a custom compressed-air launcher, as illustrated in Figure 4. The cannon was barreled to the size of a regular tennis ball, and it was possible to launch one or two simultaneously. Three avian species (two offshore, one onshore) of regulatory concern include the marbled murrelet (*Brachyramphus marmoratus*), the short-tailed albatross (*Phoebastria albatrus*) and golden eagle (*Aquila chrysaetos*). They reflect a wide variety in body length and weight of 24 cm and 202 g for the murrelet, 70 cm and 3600 g for golden eagle, to 91 cm and 4680 g for the albatross. Specific bat species that were investigated include the hoary and silver-haired bats. They have body length of 11-15 cm and weight of 10-30 g. All species can fly at speeds up to 45 km/hour or more. When considering the impact kinetics, it is more likely that a bird/bat would be hit by the leading edge of a blade than the animal running into the rapidly moving face of the blade (up to 250 km/hr or more). Additionally, the tennis balls were launched from ground and flying in a parabolic trajectory before hit by the blade. Therefore, the impact kinetics is more a function of the object mass and the blade speed. Tennis ball mass was 57 g without water, and 140 g when filled with water, which is comparable to small birds or large bats. In addition, tennis balls were easy to launch and made no damage to the blade. Launch direction in reference to the rotor was downwind in the case of NAWRTC and upwind in the case of NREL-NWTC. Regulations at NREL prevented launching of balls from downwind toward the rotor, which at the NAWRTC allowed two passes to be made through the rotor, for medium and high wind, effectively doubling the probabilities of a blade strike.

Due to varying wind conditions, low impact rate, and short timeframe of field testing, a limited number of collision events was created and recorded. During field testing, the ring buffer duration was set for 10 s before and after impact of the tennis ball. All recordings were manually triggered to ensure that data are collected for later examination and post-processing. Field notes of visually observed impact events including time, position of impact, blade status, and weather conditions were taken and matched with output data acquired from each sensor node. Typical accelerometer and contact microphone data post-processing included 1) First stage with visual inspection of time histories for quality control purposes and for event detection, and 2) Second-stage processing including numerical signal analysis.

Figure 4: Air cannon is used to launch tennis balls to mimic bird impacts at NREL-NWTC.

In summary, a total of 23 dynamic impact (i.e. tennis balls hitting moving blades) events were successfully obtained at NAWRTC, and six were obtained at NWTC under wind turbine normal operating condition (i.e. rotor at designed speed, generator engaged). The higher impact rate at NAWRTC was primarily caused by more favorable wind conditions. Likewise, four additional dynamic impact events were recorded at NWTC under turbine idle operation (i.e. blade free spinning, generator not engaged) due to low wind occurrence. The signal-to-noise ratio (SNR) was defined as follows:

$$\mathrm{SNR} = 20log_{10}\frac{A_{\mathrm{impact}}}{A_{\mathrm{noise}}} \tag{1}$$

where A is the root mean square (RMS) amplitude, and was calculated and evaluated for all impacts.

3 Results and discussion

3.1 Signal quality of vibration node

Figure 5 shows a sample of the six time histories vibration data (two sensors per blade, three blades) collected at NAWRTC, which resulted from a single impact of a tennis ball on one blade. Signals from accelerometers are in the left column, with sensors labeled N543, N648, and N649, respectively. Signals from the three contact microphones are in the right column, with the sensors labeled A, B, and C. Although the ball was struck by one blade only, it is evident from the figure that two accelerometers and all three contact microphones had picked up the impact, demonstrating the generally higher sensitivity to impact detection of contact microphones. In our specific case, however, the wireless transmission protocol for the accelerometers was decisively more reliable than the contact microphones, resulting in an unpredictable and relevant loss of data for the latter system. Therefore, the choice of the accelerometers was

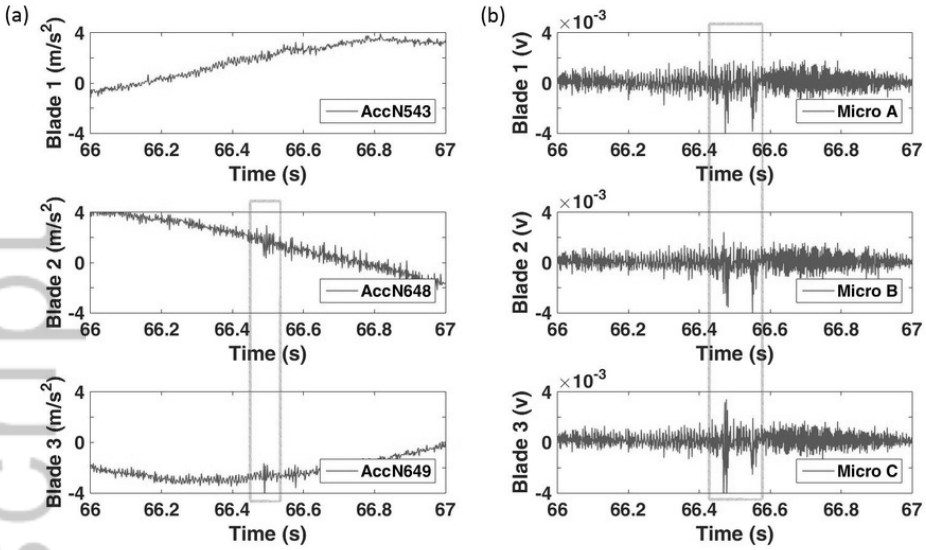

Figure 5: Sample time history plots showing vibration data collected by all six sensors (two sensors per blade, three blades) from a single impact event on one blade at NAWRTC for (a) accelerometers and (b) contact microphones. The impact can be identified through visual inspection on two accelerometers and three contact microphones.

the primary source of vibration data for post-processing and statistical analysis in the present work. In addition, the contact microphone exhibited consistently noisy signals, resulting in random false positive impact information. The wireless protocol of the accelerometers included a signal storage capability at the sensor level and a feature for automatic transmission repetition of data packets in the event of a lost connection.

3.2 Configuration of optical node

Using the target resolution simulation, the spatial coverage, which is defined as the percentage ratio between the camera surveillance area and the area of the blade rotor plane, as well as the target pixel resolution, was estimated using the turbine at the NREL-NWTC as reference (rotor diameter of 40 m and nacelle length of 9 m). As an illustration, the camera was positioned at the rear end of the nacelle looking forward toward the rotor at an angle of 55° upward from the horizontal plane. For an image resolution of 640x480 pixels and a focal length of 12 mm, Figure 6 shows a contour plot of pixel density for a target with dimensions of 240x240 mm on the rotor plane, assuming the target was struck by the blade. In this configuration, the camera provided a spatial coverage of 6.5% and minimum target resolution of more than 100 pixels. Three different camera positions, at the end of the nacelle, at the tower base, and on an adjacent tower at a distance of 200 m from the turbine, were evaluated using the same simulation model. Results, which are summarized in Table 1, illustrate spatial coverage and target resolution for a standard 240x240 mm object. As expected, the relation is inverse between camera coverage and image pixel resolution. The configuration on an adjacent tower provides more than 90% coverage at the expense of target resolution to a mere

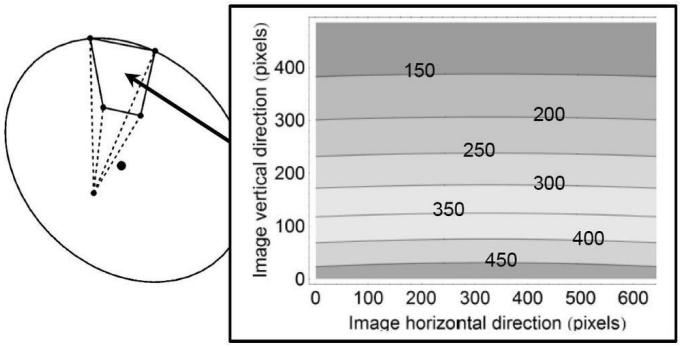

Figure 6: Contour plot of target resolution for single camera deployed on the nacelle.

Table 1: Computational results of spatial coverage and target resolution for different camera configurations.

Camera location	Spatial coverage	Minimum target resolution (a 240x240 mm target)
On the nacelle	approximately 7%	more than 100 pixels
Near the tower base	approximately 50%	more than 50 pixels
On adjacent tower	approximately 90%	less than 20 pixels

20 pixels. The camera placed at the tower base offers up to 50% of coverage with a medium pixel density of 50. The negative characteristic of the above positions is the inability of the camera to follow the yawing of the nacelle, an impractical solution.

3.3 Impact-driven architecture

Validation of the blade sensor-triggering capabilities was critical for system characterization. Simulations of blade collision events using tennis balls were conducted along different sections of the rotating blades during field testing. An example of a blade striking a tennis ball is also illustrated in Figure 7, showing the signal from the accelerometer mounted on the blade. The three time histories represented from top to bottom are 1) NREL CART3 during normal operations producing energy, 2) NAWRTC GE during normal operations producing energy, and 3) NREL CART3 during idle with generator disengaged. Table 2 lists the results of average SNR and the corresponding coefficient of variation (CV) for each testing case. In all three plots in Figure 7, the noise in the signals correspond to the vibrations on the root of the blade, measured by the accelerometer. The spikes of impact were slightly ahead of the triggering events due to the reaction time of the recorder. As expected, idle operations, shown in the bottom plot in Figure 7, are characterized by a lower background vibration noise which results the highest SNR due to the disengagement of the generator and low-power operation of the gearbox. In addition, Figure 7 and Table 2 reveal the generally lower background vibrations on the GE turbine with respect to the NREL CART3; this condition of higher SNR would improve the efficiency of data post-processing. The problem of automatically detecting a blade impact in the presence of noise at various, but predictable, frequencies could be solved by applying time-frequency analysis

Table 2: Overview of signal-to-noise ratio for all impacts

Cases	Number of impacts	Average SNR (dB)	CV (%)
CART3 600 kW normal operation	6	5.45	35.74
CART3 600 kW idle operation	4	14.59	37.01
GE 1.5 MW normal operation	23	7.03	33.05

techniques, a common procedure in analyzing vibrations from rotating machines. The short-time Fourier transform (STFT) was applied to the accelerometer signals in second-stage data post-processing. The primary result of this method, a spectrogram, is illustrated in Figure 8. The spectrogram provides a visual representation of the frequency spectrum in the time window selected for post-processing. The technique was chosen for the potential application to detect impacts in real time. The example given in Figure 8 is the spectrogram obtained from the signal of the accelerometer installed on a blade of the NREL CART3 turbine during idle operation with the blade hitting a tennis ball. The time history of the same event is illustrated on the left of Figure 8; it shows the acquired signals from the accelerometer with time on the vertical axis. The spectrogram exhibits a spike in the frequency domain at the time of the blade hitting the tennis ball, thus unequivocally identifying the strike. Frequency levels at different times represent typical turbine background vibrations due to blade aerodynamics, structural vibrations, bearings, gearbox, and various mechanical sources.

General results from 29 field tests with blade strikes showed the positive detection and confirmation of 14 events. The most probable cause of partial impact detection was the low-energy aspect of several events, with the result of a significantly low sensor signal-to-noise ratio that cannot be detected with the current post-processing technique. Most of the detected strikes occurred at the leading edge of the blade and in a radial position between half blade and blade tip, thus at relatively high kinetic energy. Impacts during turbine idle operations are particularly favorable for detection due to the extremely low background noise measured by the sensors. A result of great interest was the capability of detecting a strike of a blade to a tennis ball by any of the sensors installed on the three blades, an indication that not necessarily all blades of a rotor need to be provided with sensors to detect impacts.

4 Conclusions

This study demonstrates through experimentation the feasibility of an impact detection system based on vibration sensors that are integrated into a multi-sensor array to detect and identify causes of blade impacts on wind turbines. Our study also highlights the necessity to validate any impact detection system by operating field tests on full-scale wind turbines in real operating conditions and by simulating bird impact on the blades. Results from this study elucidate several key characteristics and critical features for efficient automatic impact detection on wind turbine blades. The system can be adapted easily to any structure exposed to impact events. Cameras for impact confirmation

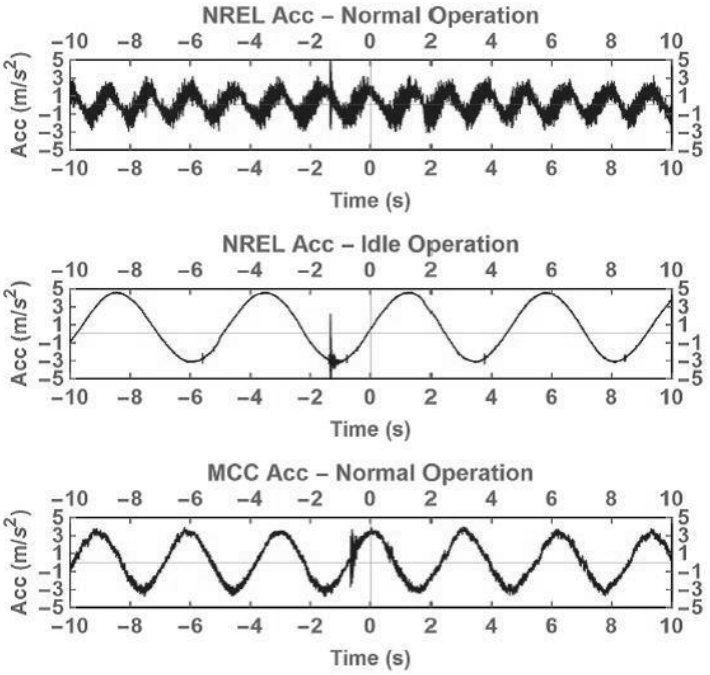

Figure 7: Accelerometer data from the CART3 600 kW turbine during normal operation and idle operation, and the GE 1.5 MW turbine during normal operation from top to bottom. Impacts were measured and can be seen on the plots at -1.33, -1.30 and -0.6 seconds, respectively.

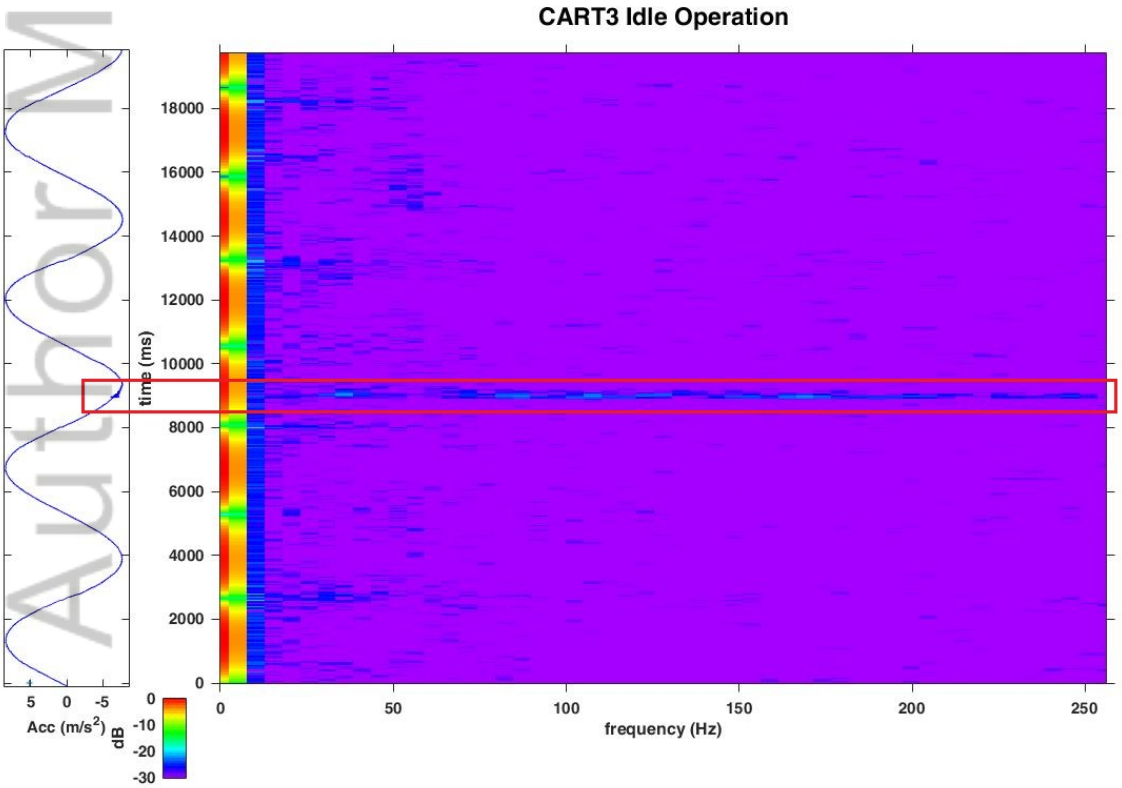

Figure 8: Illustration of acquired vibration data post-processing using STFT. The plot on the left shows the time history signal of the accelerometer installed on a blade of the CART3 turbine during idle operation. An impact was identified by its corresponding spectrogram, which exhibits a spike in the frequency domain.

and animal species recognition are critical, however, camera installation on the nacelle or any other fixed structure on or around the wind turbine has little practical value for the significantly small field of view with the minimum pixel density required for species recognition. Automatic triggering of the cameras using vibration sensors on the blades is an efficient technique, providing the sensors have a reliable wireless data transmission, a high signal-to-noise ratio and, most important, an efficient and fast post-processing technique to discern the spike caused by the impact from the normal vibration background. Using a combination of visual impact detection by inspecting vibration signal time histories and running short-time Fourier transform, 14 out of 29 registered artificial impacts were detected, which corresponds to a 48.3% success rate. Considering a more efficient automatic detection event from vibration sensors, it is strongly believed that the success rate can be significantly increased. It is important to note that several impacts were successfully detected by sensors installed on blades other than the blade subjected to the impact. This is an indication that only one or two blades, out of three, could be instrumented with vibration sensors without decreasing the detection success rate significantly. However, it is required to have all three blades in the vision system field of view for event confirmation and animal species recognition. It was evident from the field tests that contact microphones have greater potential than accelerometers in terms of sensitivity and ease of signal processing. However, the low quality of wireless transmission of the available commercial contact microphones has hampered their use, and results from accelerometers were used primarily for impact detection. Bioacoustic microphones embedded in the system, providing they can record a signal relatively clean from background noise, can have a significant value in terms of event confirmation, can enhance species recognition in the presence of animal calls, and provide information on environmental variables affecting sensors such as rain, lightning, etc. Micro wireless visual sensors mounted directly on the blades have been tested briefly, with great success in terms of blade impact area coverage, species recognition, and potential for event detection.

5 Future work

With the general aims of improving automatic real-time impact detection, increasing video imaging coverage, and decreasing system energy requirements, the following improvements are suggested:

- Blade vibration sensors should have on-board data processing capabilities and transmit a packet of data only after the impact is detected;
- Sensor fusion should be applied to improve detection success rate;
- Sensor wireless transmission should rely on more efficient and standard wireless protocols;
- An efficient and fast event detection method should be applied, possibly with real-time signal filtering to decrease background noise and improve the detection success rate;

- Micro wireless visual sensors should be mounted directly on the blades to greatly increase critical impact area coverage;
- More tests should be carried out with the specific objective to establish the minimum number of vibration sensors on blades required for camera triggering;
- Micro infrared camera mounted on blades should be tested for night vision;
- Solar energy or rotational motion energy harvesting for sensor battery charging should be tested for increased autonomous and low-maintenance operations.

6 Acknowledgments

The authors wish to acknowledge the financial support of the U.S. Department of Energy under DE-EE0005363. The authors are grateful to the staff of the North American Wind Research and Training Center at Mesalands Community College for contributing to the success of the systems first field test. The authors would also like to express gratitude to the staff and scientists at NREL for their willingness to share information with the team and for use of the Controls Advanced Research Turbines at the National Wind Technology Center for system testing and demonstration. Finally, we greatly appreciate the review and expert contributions of our science and industry advisory panel.

References

1. Schwartz M, Heimiller D, Haymes S, Musial W. *Assessment of Offshore Wind Energy Resources for the United States*. NREL/TP-500-45889; 2010.
2. Bailey H, Brookes KL, Thompson PM. Assessing environmental impacts of offshore wind farms: lessons learned and recommendations for the future. *Aquatic Biosystems*. 2014;10(8).
3. Thomsen K. *Offshore Wind: A Comprehensive Guide to Successful Offshore Wind Farm Installation*. London: Elsevier Science; 2014. ISBN 9780124095946.
4. Flowers J, Albertani R, Harrison T, Polagye B, Suryan RM. Design and Initial Component Tests of an Integrated Avian and Bat Collision Detection System for Offshore Wind Turbines. In: Marine Energy Technology Symposium; April 15–18, 2014; Seattle.
5. Sovacool BK. Contextualizing avian mortality: A preliminary appraisal of bird and bat fatalities from wind, fossil-fuel, and nuclear electricity. *Energy Policy*. 2009;37(6):2241–2248.
6. Marques AT, Batalha H, Rodrigues S, Costa H, Pereira MJR, Fonseca C, Mascarenhas M, Bernardino J. Understanding bird collisions at wind farms: An updated review on the causes and possible mitigation strategies. *Biological Conservation*. 2014;179:40–52.
7. Kunz T, Arnett EB, Cooper BM, Erickson WP, Larkin RP, Mabee T, Morrison ML, Strickland MD, Szewczak JM. Assessing Impacts of Wind-Energy Development on Nocturnally Active Birds and Bats: A Guidance Document. *Journal of Wildlife Management*. 2007;71(8):2449–2486.

8. Sovacool B, Lindboe HH, Odgaard O. Is the Danish Wind Energy Model Replicable for Other Countries?. *Electricity Journal*. 2008;21(2):27–38.

9. Plonczkier P, Simms IC. Radar monitoring of migrating pink-footed geese: behavioural responses to offshore wind farm development. *Journal of Applied Ecology*. 2012;49(5):1187–1194.

10. Brabant R, Vanermen N, Stienen EWM, Degraer S. Towards a cumulative collision risk assessment of local and migrating birds in North Sea offshore wind farms. *Hydrobiologia*. 2015;756:63–74.

11. Fijn RC, Krijgsveld KL, Poot MJM, Dirksen S. Bird movements at rotor heights measured continuously with vertical radar at a Dutch offshore wind farm. *Ibis*. 2015;157(3):558–566.

12. Towsey M, Wimmer J, Williamson I, Roe P. The use of acoustic indices to determine avian species richness in audio-recordings of the environment. *Ecological Informatics*. 2014;21:110–119.

13. Masden EA, Cook ASCP. Avian collision risk models for wind energy impact assessments. *Environmental Impact Assessment Review*. 2016;56:43–49.

14. Marquez FPG, Tobias AM, Perez JMP, Papaelias M. Condition monitoring of wind turbines: Techniques and methods. *Renewable Energy*. 2012;46:169–178.

15. Abouhnik A, Albarbar A. Wind turbine blades condition assessment based on vibration measurements and the level of an empirically decomposed feature. *Energy Conversion and Management*. 2012;64:606–613.

16. Bassett K, Carriveau R, Ting DS. Vibration response of a 2.3 MW wind turbine to yaw motion and shut down events. *Wind Energy*. 2011;14(8):939–952.

17. Wiggelinkhuizen EJ, Rademakers LWMM, Barhorst SAM, Boon HJ, Dirksen S, Schekkerman H. WT-bird: Bird collision recording for offshore wind farms. In: European Wind Energy Conference; Feb. 27–Mar. 2, 2006; Athens.

18. Desholm M, Fox AD, Beasley PDL, Kahlert J. Remote techniques for counting and estimating the number of bird wind turbine collisions at sea: a review. *Ibis*. 2006;148(s1):76–89.